Aerosol and Air Quality Research, 12: 304–319, 2012

ISSN: 1680-8584 print / 2071-1409 online
doi: 10.4209/aaqr.2011.11.0200

Study on Long-term Aerosol Distribution over the Land of East China Using MODIS Data

Qianshan He[1], Chengcai Li[2*], Fuhai Geng[1], Yong Lei[3], Yuhong Li[4]

[1] *Shanghai Meteorological Bureau, 166 Puxi Road, PO Box 200030, Shanghai, China*
[2] *Laboratory for Climate and Ocean-Atmosphere Studies, Department of Atmospheric and Oceanic Sciences, School of Physics, Peking University, PO Box 100871, Beijing, China*
[3] *Meteorological Observation Centre, China Meteorological Administration, 46 South Zhongguancun Avenue, PO Box 100089, Beijing, China*
[4] *Shanxi Meteorological Bureau, 45 Xinjian Road, PO Box 030002, Taiyuan, China*

ABSTRACT

East China is among the fastest developing area in Asia, where atmospheric aerosol loading is high due to heavy urban and industrial emission. The Moderate Resolution Imaging Spectroradiometer (MODIS) level 2 aerosol products (2000–2007) were used to study aerosol spatial and temporal distributions, as well as their variations with local meteorological conditions over East China. By combining Aerosol Optical Depth (AOD) and aerosol Fine Mode Fraction (FMF), we found that the urban/industrial aerosol and soil dust are possibly two dominant species over northern part, whereas continental and marine aerosols possibly dominate the southern part of East China. Both annual mean AOD and area with high AOD increased from 2000 to 2007, with the largest increase seen in Yangtze River Delta region (YRD). In summer, AOD in East China reached the maximum of about 0.8 in YRD, dominated by fine mode particles. The minimum AOD occurred in winter with mostly coarse mode particles. Local aerosol properties were analyzed in three typical zones: the northern dry zone (I), the central urban/industrial zone (II) and the southern natural background zone (III). Monthly mean AODs in zone I and II were above 0.5 throughout the entire year, with the maximum AOD in June. High FMFs in this period indicated heavy urban and industrial pollution. Monthly mean AODs and FMFs in zone III reached maximum of 0.51 in April and September (up to 90.7%) respectively. High AOD in spring in zone III appears mostly due to the long-range dust transport from the North.

Keywords: Aerosol; MODIS; East China; Remote sensing; Optical properties.

INTRODUCTION

Aerosols are a major factor affecting Earth's radiation budget and hydrologic cycle. They affect climate through direct interactions with solar and terrestrial radiation (direct aerosol effect), and through their effect on the optical and microphysical properties and lifetime of clouds (indirect aerosol effect) (Charlson *et al.*, 1992; Levine *et al.*, 1995; Haywood and Boucher, 2000). Atmospheric aerosols in high concentrations can also affect human health and reduce visibility. The biggest uncertainty in climate change, even by the best available General Circulation Models, is due to uncertainties in aerosol radiative forcing (IPCC, 2001). This uncertainty arises mainly because of our poor understanding on both aerosols' temporal and spatial distributions and their associated properties (Pilinis *et al.*, 1995). In order to carry out model studies of the global climate change, studies of aerosol properties at different locations are essential to our understanding of the recent climate change (IPCC, 2001).

Different techniques are available to measure spatial and temporal variations of aerosols. On a global scale, remote sensing instruments such as MODIS on aboard both polar orbiting TERRA and AQUA satellites continue to produce global AOD maps retrieved from backscattered solar radiation through the atmosphere (King *et al.*, 1992; Kaufman *et al.*, 2003; Levy *et al.*, 2003; Hutchison *et al.*, 2005; Tang *et al.*, 2005). These satellite-based remote sensing techniques offer a much wider spatial view than in-situ or surface-based radiometric observations. Satellite-retrieved AOD can be a useful parameter for the estimation of optical and physical characteristics of aerosol on the regional scale. Recently, MODIS-derived aerosol properties have enabled us to comprehensively study the spatial and temporal variations of aerosols (Barnaba and Gobbi, 2004; Chu *et al.*, 2005).

East China is a fast developing and densely populated region in the world, and a major source of aerosol emissions

* Corresponding author. Tel.: 86-10-6276-2552;
Fax: 86-10-6275-1094
E-mail address: ccli@pku.edu.cn

where loadings are high and chemical/physical properties are complex (Li, 2004). A handful of field experiments have been conducted in this region such as the Asian-Pacific Regional Aerosol Characterization Experiment (ACE-Asia) (Huebert *et al.*, 2003) and the Asian Atmospheric Particle Environment (APEX) (Nakajima *et al.*, 2003). Luo *et al.* (2001) analyzed AOD at 750 nm observed from 46 stations in China and concluded that the middle and back drainage area of YRD has been characterized by most distinct AOD increase since 1980s. Many cities in East China experienced high airborne particle concentrations emitted from biomass burning, motor vehicle exhaust, as well as secondary sulfates formed from the sulfur dioxide by atmospheric chemical reactions. Heavy aerosol loading in this region has been reported based on ground and satellite instruments (e.g. Xiao *et al.*, 2011). Regional temperature and precipitation pattern changes from the mid-1970s were suggested to be related to the heavy aerosol loading and aerosol's strong absorption in East China (Qian and Giorgi, 2000; Xu, 2001; Menon *et al.*, 2002). Using data from Geostationary Meteorological Satellite (GMS), Zhang *et al.* (2003) found relatively higher AOD in the middle and back drainage area of YRD and coastal region in East China. Xu *et al.* (2002) analyzed aerosol chemical/physical and radiative data observed in Lin'an, Sheshan and Changshu city of YRD in 1999, and found that the aerosol radiative properties in Lin'an, a typical rural background, showed more urban rather than rural characteristics.

The underlay characteristics of East China are complicated with coasts, plains and mountains. The temperature, precipitation and relative humidity vary largely with different seasons, and can significantly influence the temporal and spatial distributions of aerosols. The growing population and transportation in East China has resulted in high demands on energy. Aerosol from urban/industrial emissions, dusts, and sea salt brought by wind all contribute jointly to the regional aerosol loading. Furthermore, agricultural biomass burning aerosols can also be transported into East China from the surrounding rural area in June (Lee *et al.*, 2006; Li *et al.*, 2010).

In the previous studies, most of the aerosol characteristic over east China was studied using observation data (such as sunphotometer) from discrete sites. The long-term continuous observation for the spatial and temporal distribution of aerosol from satellite was scarce. It should be noted that climate simulation should take consideration of this complicated spatial and temporal variations of aerosols distributions due to rapid economic growth. The climatologic mean value was incapable to describe precisely the effect on regional climate and environment change induced by aerosol and so more detailed and high spatial and temporal resolution aerosol information is necessary. In this paper, we synthesize the multi-year datasets of column-integrated aerosol optical and physical properties obtained from satellite sensor MODIS to investigate regional aerosol characteristics over East China. We considered four seasons: spring (MAM) (dry and dusty), summer (JJA) (rainy and accounts for about two-thirds of the annual precipitation), autumn (SON) (dominated by anticyclone), winter (DJF) (windy, sunny and dry). Parameters used in this study include AOD at 550 nm, Angstrom exponent (α) and FMF. All products are given at a spatial resolution of 0.1° × 0.1°. The FMF is defined as the ratio of optical depth (550 nm) of fine-mode particles to that of total aerosols at 550 nm based on the assumption of bi-modal lognormal size distributions.

MODIS AEROSOL ALGORITHM AND GEOGRAPHICAL AND CLIMATIC CHARACTERISTICS

MODIS AOD retrieval over land employs primarily three spectral channels centred at 0.47, 0.66, and 2.1 μm. AOD is derived over land at 0.47 and 0.66 μm, and interpolated to 0.55 μm. More details about the retrieval algorithm are presented in the literatures by Kaufman *et al.* (1997) and Remer *et al.* (2005). The major error sources of MODIS derived AOD are the assumed constant ratio between surface reflectivity at 2.1 μm and that at visible wavelengths. In order to improve the retrieval accuracy, the second-generation operational algorithm performs a simultaneous inversion of two visible (0.47 and 0.66 μm) and one shortwave-IR (2.12 μm) channel, considers the influence of scattering angle (including solar zenith angle, viewing zenith angle), surface type and NDVI to the assumed surface reflectivity relationship. The new algorithm also replace the assumed aerosol mode optical properties with the multi-year measurement from AERONET. Preliminary validation of this algorithm shows much improved retrievals of AOD, where the MODIS/Aerosol Robotic Network (at 0.55 μm) correlation coefficient is up to 0.90 (Levy *et al.*, 2007).

FMF of AOD, is determined from the spectral dependence of the path radiances at 0.66 and 0.47 μm (Kaufman *et al.*, 1997; Remer *et al.*, 2005), provides an indication of whether the AOD is dominated by fine mode or coarse mode aerosols. The fine mode aerosols over urban, industrialized and densely populated regions are mainly due to the gas to particle conversion (fossil fuel, biomass combustion-anthropogenic), while coarse mode aerosols such as windblown mineral dust and sea salt particles mainly arise from natural sources (Ramachandran, 2007). A comparison of MODIS and AERONET remote sensing retrievals of aerosol fine mode fraction over ocean surfaces showed that MODIS slightly overestimates fine mode fraction for dust dominated aerosols, while it underestimates in smoke and pollution dominated aerosol conditions (Kleidman *et al.*, 2005). Ramachandran (2007) validated and compared MODIS derived FMFs with monthly mean in situ AERONET measurements over Kanpur in north India, and found a good agreement during most of the months. Additionally, Kim *et al.* (2007) employed MODIS/Terra aerosol products (including AOD and FMF) to analyze the temporal and spatial variability of aerosols over East Asia. These validations and applications illustrate that MODIS aerosol products (AODs, FMFs) can be used to study the spatial and temporal variations in aerosol characteristics as the MODIS derived AODs and FMFs capture the major part of seasonal variations and the dominant aerosol type. Barnaba and Gobbi (2004) have presented a simple method for classifying main aerosol types from MODIS data but they didn't consider biomass burning and

urban/industrial aerosol. Dubovik *et al.* (2002) investigated the aerosol optical properties obtained from sun photometers located in several typical sites and found that the averaged AODs (440 nm) of the biomass burning aerosol are 0.75 and 0.39 in Brazil and North America respectively. Xia *et al.* (2006) employed the AERONET data and in situ measurement to analyze aerosol properties in Beijing and found that aerosol size and absorption in this Chinese urban region are close to results derived in Mexico City and Kanpur, but they are quite different from those in Maryland and Paris.

We used the 10 × 10 km MODIS derived AODs and FMFs from the second-generation operational algorithm product (C005) to obtain the monthly mean values over East China, and then the annual and 8-year mean values.

East China ranges from the mid-latitudes to the subtropical zone, with complicated topography characterized by mostly plains in the northern part, and mountains in the southern part. Fig. 1 gives the location of East China with topography. Anhui Province, a territory in the northern part, has the largest coal storage and steel industry in China. The Yangtze River, the longest river in China, traverses East China region and flows into the East China from west. Cities with more than one million in population include Shanghai (one of the largest city in the world), Nanjing, Hangzhou, Suzhou, Wuxi, Ningbo, Changzhou, Jinan, Hefei, Nanchang and Fuzhou. Most of these cities are located in the Yangtze River Delta region, whose gross industrial output value account for nearly 1/4 in China.

Divided by the Yangtze River, the northern and southern parts of East China are controlled by different climate zone. The northern part is in the transition zone from warm temperate monsoon region to subtropical climate, characterized by uneven seasonal precipitation distributions. The 60–70% of its annual precipitation occurs between June and August, with the Plum rain and the Autumn rain (also tropical cyclones) as the main contributors. The Plum rain, a typical weather in middle and lower reaches of the Yangtze River region, usually starts in mid-June and ends in earlier July. Monsoon changes significantly with different seasons. In winter, this region is controlled by the Mongolia high pressure and the Aleutian low pressure, and influenced by frequent cold air invasion from the north. This results in the prevalence of the north-westerly and north-easterly winds with cold and dry weather. In summer, continental heat low pressure produces the prevailing south-easterly wind with warm and humid weather. The Northwest Pacific subtropical high dominants in July and August and sometimes brings

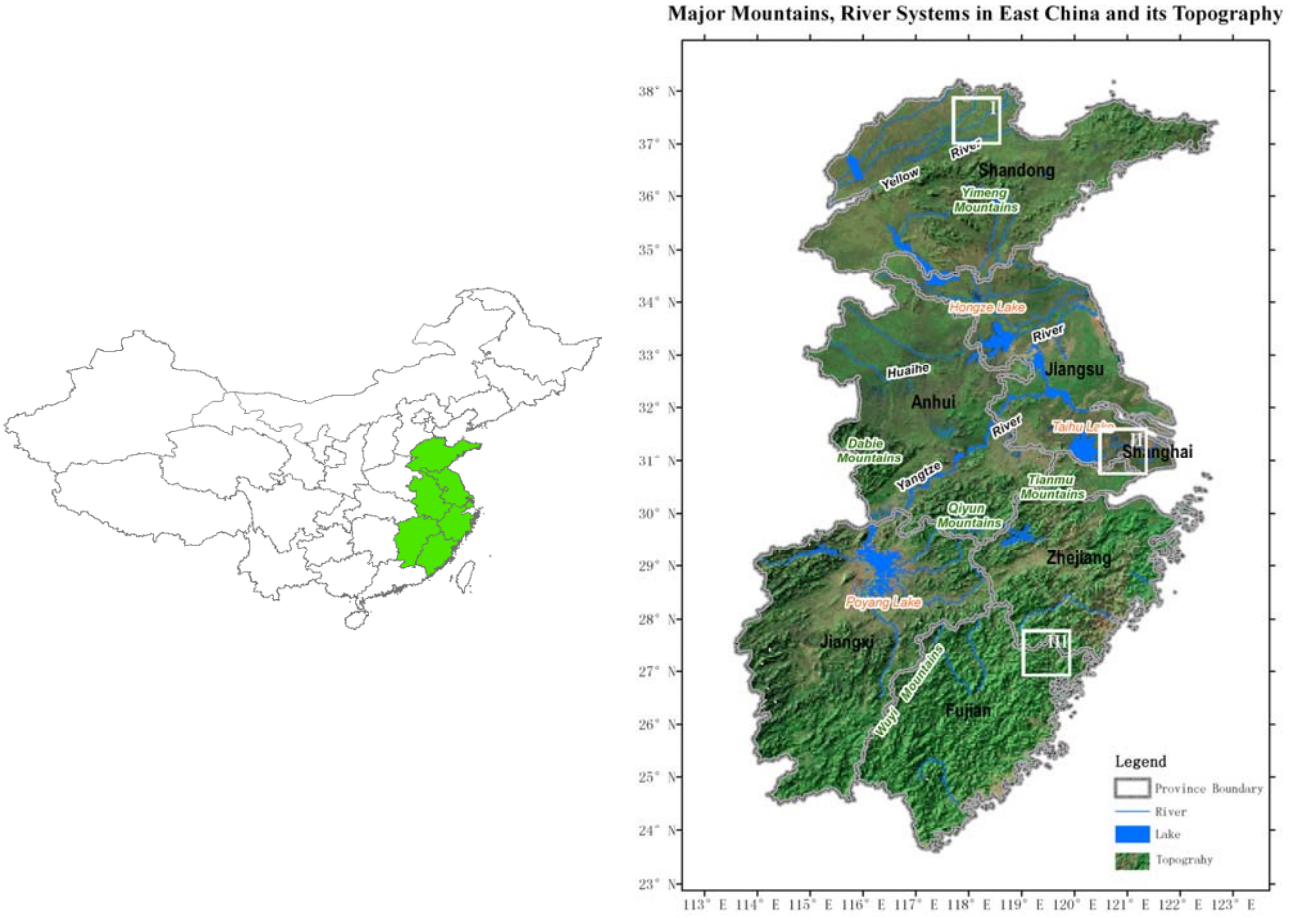

Fig. 1. The location and terrain of East China. The rectangles with Roman number are the location of three typical zones with each area of 100 × 100 km^2 in East China according to their aerosol source and local meteorological condition. The Roman numbers in the frame are the name of the zones.

hot and dry air. North-easterly and easterly winds usually prevail in spring and autumn, bringing frequent cold and wet condition and convection. The southern part is a typical subtropical monsoon climate zone, affected by the East Asian monsoon, with seasonal changes in prevailing wind direction and precipitation amount. In spring, the northerly and southerly flows switch frequently. In summer, this region is controlled by the prevailing southeast wind and the northwest Pacific subtropical high activities. In autumn, frequent cyclones lead to abundant precipitation. In winter, the dominant northerly wind is usually companied by dry, cold weather. More than 50% of the annual precipitation occurs from April to July (Yuan and Qian, 2003).

RESULTS AND DISCUSSION

Summary of Aerosol Distributions in East China

AOD and α over East China from MODIS are averaged from 2000 to 2007 and shown in Fig. 2. Areas in East China with high AOD are found in the densely populated and industrialized areas (individual cities and clusters of cities). Very high values are found in the northwest plain in Shandong province, Huanghuai, Poyang Lake Plain and the Yangtze River Delta region (especially in areas along the Yangtze River). Some small scale features, such as major cities (Nanjing, Shanghai) can be distinguished. Low AOD values are observed in southern part and over the mountains throughout East China (Wuyi cordillera, etc.). Clearly, most aerosols are detected being close to their source regions. As a highly urbanized area with dense population and developed industry, the Yangtze River Delta is characterized by a rich aerosol emission region. North-western Shandong plain has lower urbanization compared with YRD, but it is vulnerable to dust transported from North China. In addition, the Yimeng cordillera on the eastern Shandong province blocks the west flow, resulting in aerosol accumulation along nearby western border of the cordillera. Aerosol distributions in Huanghuai region also strongly depend on topography and industry locations. The Yangtze River valley in Anhui Province was surrounded by Dabie and Tianmu cordillera. It has several cities with more than one million population and numerous copper smelting industry and coal bases. Aerosols emitted in this region are hard to be dissipated. On the other hand, this region is one of the main channels of aerosol transport from the west. Poyang Lake plain, surrounded by the mountains, suffers severe aerosol accumulation due to the basin effect and high anthropogenic emission.

α depends on the size of the aerosol particles. It is small for coarse particles and increases with decreasing particle size. According to MODIS, α ranges from 0 to 1.8 for the most parts of East China, but appears to be lower over the northern part than the southern part. α is anti-correlated with AOD (r~0.79), which indicates that the increasing AOD over the northern part of East China is mainly caused by those aerosol particles with large size like dust-like aerosols and windblown dust, possibly produced by more frequent construction activities and poor vegetation cover condition in this region (He *et al.*, 2006). In East China, the smallest α values are usually located in coastal areas and the largest α values (> 1.6) are usually located in Tianmu cordillera in Zhejiang, Qiyun cordillera in Jiangxi and Hawksbill cordillera in Fujian. The α varies in the range

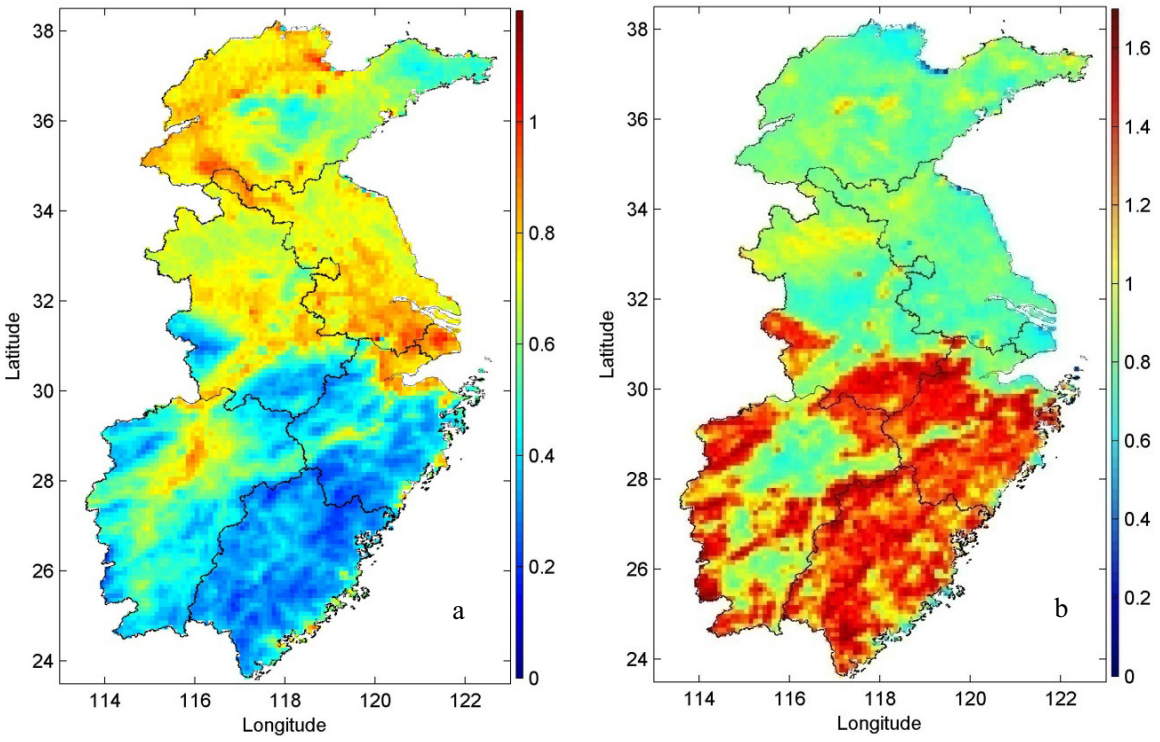

Fig. 2. The distribution of (a) AOD and (b) α over East China averaged from MODIS level 2 products in the period of 2000–2007.

between 0.6 and 1.0 in the northern part of East China and the Poyang Lake plain. However, caution must be taken here that α is even more sensitive to the assumptions on the spectral dependence of the land surface than the AOD, followed by uncertainties of aerosol properties (such as particle size and ω_0). He *et al.* (2010) compared MODIS derived α with sunphotometer CE318 measurements from 7 sites located at YRD in East China from July to October, 2007. They divided all MODIS derived α samples into two categories according to air flow sources in order to further clarify the influencing factors of MODIS derived α. One represents the inland aerosol particles, the other for marine particles. Meanwhile, they found that the MODIS derived α is more dispersed from marine aerosol whose correlation coefficient is 0.07, when its correlation coefficient is 0.37 from land aerosol.

Possible Distribution of Aerosol Types

Fig. 3 presents the distribution of FMF over East China averaged from MODIS level 2 products in the period of 2000–2007. The spatial distribution of FMF is similar to that of α with lower values located in the north part of East China and higher ones in south. The very small FMF (< 20%) located the centre part of Anhui and the north part of Shandong, while the contribution of fine and coarse particles to aerosol properties is almost uniform in the most district of north part in East China with FMF between 40% to 60%. According to the AOD~FMF classification method by Barnaba and Gobbi (2004), who conclude that the aerosols with AOD (550 nm) ≤ 0.3 and FMF < 0.8 are considered to be marine type, AOD (550 nm) > 0.3 and FMF < 0.7 for dust, and all the other aerosols are considered of continental type (AOD (550 nm) < 0.3 and FMF > 0.8, or AOD (550 nm) > 0.3 and FMF ≥ 0.7), and AOD~α classification method by Dubovik *et al.* (2002), the dominant aerosols in the southern part of East China (excluding the Poyang Lake plain) are mostly emitted from natural source and possibly consist of continental and marine types, and the dominant aerosols over the northern part of East China are emitted from natural source and anthropogenic source and possibly consist of soil dust, biomass burning and urban/industrial type. The aerosols from natural source (such as soil dust) are possibly connected to the windblown mineral dust storms that usually occur in the spring (Kim, 2005). Meanwhile, plenty of construction activities due to fast economic development also contributed numerous dust-like particles into the atmosphere. The aerosols from anthropogenic source (such as urban/industrial type) over the northern part of East China are induced by numerous industry enterprises which emitted large amount of anthropogenic pollutants. This result suggests that columnar aerosol optical properties over the northern part of East China are often influenced both by dust and anthropogenic pollutants during the investigation period (Stone *et al.*, 2011).

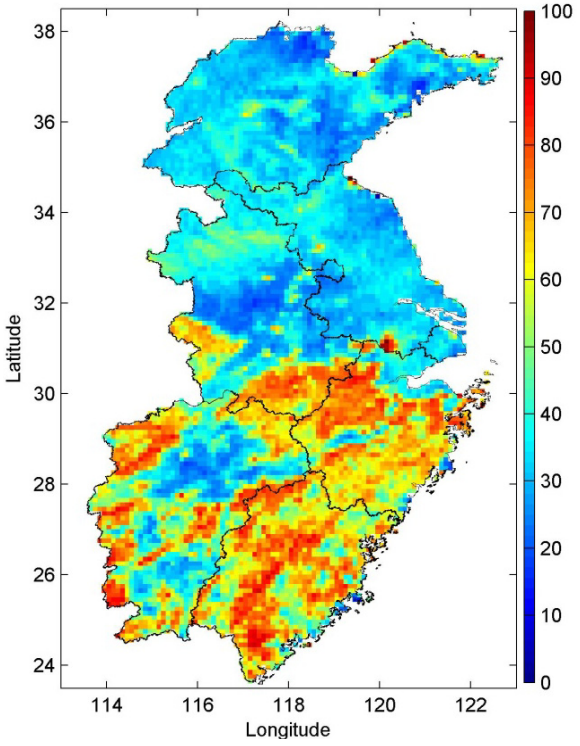

Fig. 3. The distribution of FMF over East China averaged from MODIS level 2 products in the period of 2000–2007.

Interannual Variation of AOD over East China

Annual mean AOD over East China from 2000 to 2007 are presented in this section. Several significant characteristics can be found in Fig. 4. The aerosol loading showed the increasing trend from 2000 to 2007 over East China, except in 2004 and 2005 of Shandong, when the AOD is slightly decreased compared with that in 2003. That agrees with those results by Guo *et al.* (2011), who analyzed TOMS AOD at 500 nm (1980–2001) and MODIS data (2000–2008) at 550 nm in one-degree grid over eight typical regions in China. They suggested the clear upward trend in AOD is observed from 2000 to 2008. It might be due to the increasing aerosol particles injecting into the atmosphere by the intensive industrial and anthropogenic activities over the region. Very high AOD over Shandong and YRD in 2006 possibly induced by the more frequent sand and dust storms weather and transportation in North China. There are 17 major sand and dust weather, among them there are 5 severe sand and dust storm processes transported through Shangdong province, and the number of severe sand and dust storm processed in 2006 is the most since 2000 (Zhang *et al.*, 2010).

Explosive Increasing of Aerosol Loading after 2005

Aerosol Pollution areas with AOD > 0.5 and 1.0, their proportions to the areas of different regions, such as YRD, Shandong and Anhui provinces, and pollution intensity (the mean, maximum, minimum AOD and its location) from 2000 to 2007 are listed in Table 1. Before the year of 2006, the variation of aerosol loading over East China was stable with slight fluctuation in the heavy aerosol pollution area and mean AOD. $P_{0.5}$ or $P_{1.0}$ represents the proportions of aerosol pollution area with $\tau > 0.5$ or $\tau > 1.0$ to the areas of different regions, respectively. $P_{1.0}$ were not exceed 0.5 until the year of 2006. In year 2000, the area with annual mean

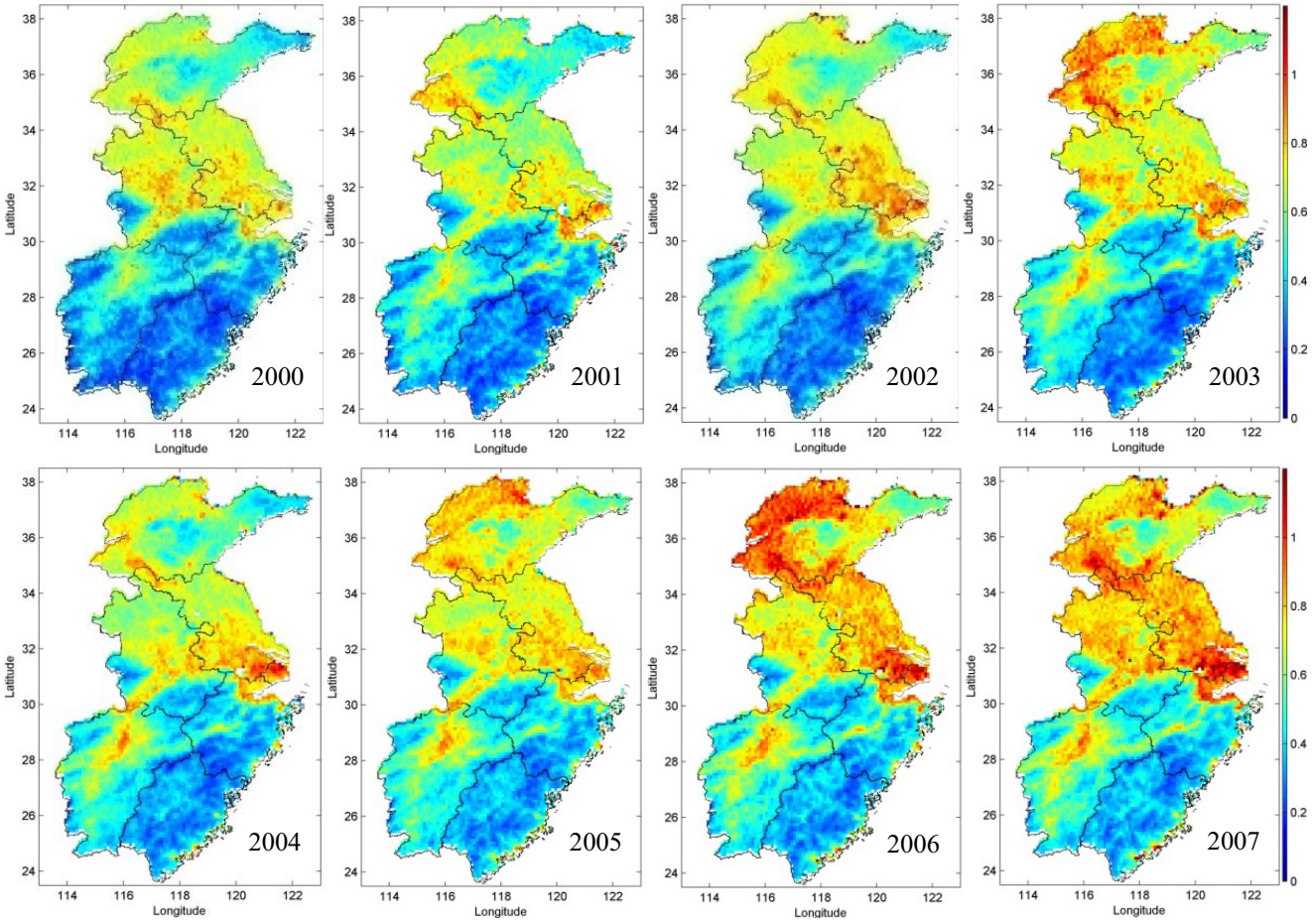

Fig. 4. The distribution of annual mean AOD over East China for 2000–2007.

AOD > 1.0 only covered a few cities along the Shanghai-Nanjing Railway. It extended to most parts of Jiangsu province and accounted for 4.3% of total area in YRD in 2007. The columnar aerosol loading increased rapidly in the year of 2007 and the area with AOD > 1.0 in 2007 was about 20 times of that before 2005. Moreover, the maximum annual mean AOD increased from 0.98 in 2001 to 2.4 in 2007, and the minimum annual mean AOD increased by 0.04 from 2001 to 2007 in YRD.

There were few areas with annual mean AOD > 1.0 before 2005, but the area (up to 70%) with annual mean AOD > 0.5 spread widely even in the cleanest year of 2001 (domain average AOD~0.58, the lowest value compared with that in other years) in Shandong province. In the most polluted year of 2006, the area with annual mean AOD > 0.5 almost covered 99.3% of Shandong province. The percentage increased up to 9.2% for the area with annual mean AOD > 1.0 with the maximum of AOD up to 1.74 in 2006.

Anhui was the cleanest province in the northern part of East China with only 500 km^2 area with AOD > 1.0, accounting for 0.4% of the whole district in 2007, which was obviously increase from zero in this year before. Similarly, the area percentage with AOD > 0.5 still increased significantly from 77.3% in 2006 to 80.6% in 2007 with the maximum AOD up to 1.14.

Among the heavy aerosol loading districts, the increment of annual mean AOD in YRD was the fastest from 2000 to 2007, where the large AOD area expanded more toward north. The peak AODs were mostly located in the big cities in northern parts of YRD from 2000 to 2007.

Inconsistent Variation of Aerosol Loading over Northern and Southern Parts of East China

Aerosol loading over the northern part increased more than that over the southern part of East China from 2000 to 2007. The South is characterized by more cordilleras, more extensive vegetation cover and less human activities, resulting in steady aerosol loading increase, except for Poyang Lake plain with slightly higher AODs. While AODs were pretty high in the North (such as the north Shanghai, Jining district in Shandong and Maanshan district in Anhui) even in the cleanest year of 2000 and 2003. Therefore, aerosol loadings in the North might associate to human activities induced constructive soil, traffic dust and industrial emissions as well as dust storms from north China (Hatakeyama *et al.*, 2011), and those in the South might associate to natural emissions.

Seasonal Characteristics of AOD over East China

MODIS-derived AOD and α presented in Fig. 5 exhibit a broad range of aerosol loading in each season as well as geographical variations. In spring, the AOD maxima appeared prominently over Huaihe district and Poyang Lake plain.

Table 1. The annual mean aerosol-related parameters in three key districts of East China.

YRD									
Year	[a]$S_{0.5}$	$S_{1.0}$	[b]$P_{0.5}$	$P_{1.0}$	[c]τ_{max}	τ_{min}	τ_{mean}	[d]L_{max}	L_{min}
2000	1.050	0.003	60.1	0.2	1.07	0.16	0.57	121.8 31.2	119.2 27.5
2001	1.079	0.000	61.8	0.0	0.98	0.17	0.56	119.3 32.8	119.1 27.8
2002	1.091	0.008	62.1	0.5	1.73	0.14	0.60	120.5 33.8	119.1 27.7
2003	1.067	0.003	60.9	0.2	1.11	0.18	0.58	122.0 31.0	120.9 33.0
2004	1.075	0.007	61.4	0.4	1.18	0.18	0.58	121.9 31.1	122.0 31.8
2005	1.124	0.003	62.8	0.2	1.16	0.22	0.60	120.0 31.2	119.1 27.8
2006	1.159	0.041	65.9	2.3	1.61	0.21	0.65	120.2 31.3	118.8 28.2
2007	1.174	0.076	66.6	4.3	2.37	0.20	0.68	118.6 33.2	119.1 27.7
All	1.132	0.003	63.2	0.2	1.13	0.20	0.61	120.0 31.2	119.1 27.8
Shandong									
Year	$S_{0.5}$	$S_{1.0}$	$P_{0.5}$	$P_{1.0}$	τ_{max}	τ_{min}	τ_{mean}	L_{max}	L_{min}
2000	1.145	0.000	74.8	0.0	0.95	0.16	0.59	118.7 37.4	122.4 37.4
2001	1.072	0.000	70.0	0.0	0.97	0.10	0.58	116.3 35.1	121.1 37.7
2002	1.326	0.007	86.6	0.5	1.98	0.28	0.64	119.5 37.1	122.6 37.2
2003	1.521	0.025	99.3	1.6	1.66	0.28	0.76	121.4 37.5	118.9 37.5
2004	1.205	0.001	78.7	0.07	1.01	0.23	0.61	118.9 37.2	122.6 37.2
2005	1.510	0.007	98.2	0.5	1.09	0.44	0.73	118.7 37.3	117.2 36.4
2006	1.521	0.141	99.3	9.2	1.74	0.44	0.81	119.2 37.1	118.2 36.3
2007	1.497	0.051	98.0	3.3	1.78	0.36	0.75	119.1 37.1	118.7 38.1
All	1.462	0.001	95.1	0.07	1.00	0.42	0.69	118.7 37.4	120.9 37.2
Anhui									
Year	$S_{0.5}$	$S_{1.0}$	$P_{0.5}$	$P_{1.0}$	τ_{max}	τ_{min}	τ_{mean}	L_{max}	L_{min}
2000	1.016	0.000	75.8	0.0	0.98	0.23	0.62	117.3 31.6	116.2 31.1
2001	1.010	0.000	75.3	0.0	0.89	0.21	0.59	118.3 31.6	118.8 30.1
2002	1.022	0.000	76.2	0.0	0.98	0.22	0.61	119.2 32.8	116.1 31.0
2003	1.045	0.000	77.9	0.0	0.98	0.23	0.64	116.9 32.2	116.1 31.0
2004	1.040	0.000	77.6	0.0	0.91	0.25	0.61	116.3 29.9	116.1 31.1
2005	1.040	0.000	77.6	0.0	0.92	0.26	0.64	116.4 30.0	118.8 30.1
2006	1.037	0.000	77.3	0.0	0.97	0.26	0.64	117.2 31.8	116.2 31.0
2007	1.081	0.005	80.6	0.4	1.14	0.26	0.70	117.6 31.5	116.2 31.0
All	1.037	0.000	77.3	0.0	0.91	0.26	0.63	117.2 31.8	118.8 30.1

[a] $S_{0.5}$ represents the aerosol pollution area with $\tau > 0.5$. The same as $S_{1.0}$ but for $\tau > 1.0$. Unit: 10^5 km^2

[b] $P_{0.5}$ represents the proportion of aerosol pollution area with $\tau > 0.5$ to the areas of different regions. The same as $P_{1.0}$ but for $\tau > 1.0$.

[c] τ_{max}, τ_{min} and τ_{mean} are the maximum, minimum and mean AOD in the study region respectively.

[d] L_{max} and L_{min} are the location (longitude °E latitude °N) of maximum and minimum mean AOD in the study region respectively.

AOD over this area is generally higher than 0.9. Over the industrialized coastal regions of YRD, the AODs are up to 0.7. The AOD maximum in summer (up to 1.0) over YRD is caused by an increase of anthropogenic aerosols, as well as a stagnant synoptic system dominated in the Asian continent, causing building up of pollutants. The aerosol particles in summer are smaller compared with other seasons as shown in Fig. 5(b), followed by that in autumn, and the aerosol particles presented largest values in spring. The seasonal variation of AOD and α derived by MODIS is consistent with those recent observations using Cimel sunphotometer data in the YRD of China (Che *et al.*, 2009; Pan *et al.*, 2010). Seasonal and spatial variations of derived AOD from MODIS were related to Asian dust and anthropogenic emission patterns in spring, but modified by precipitation in summer. Regional atmospheric dispersion by strong westerly wind dominates in autumn and winter. The westerly wind and its strength are important in transporting dust and pollutants to the downwind side of Chinese continent. The lowest AOD appeared in autumn (September–November) and winter (December–February) because aerosol loadings were strongly influenced by fast-moving synoptic weather patterns. The prevailing, strong northwesterly winds contributed to the dispersion of tropospheric aerosols. In winter, the distribution of AOD is similar to that in autumn when East China is continuously influenced by clean Asian continental air mass. The strong westerly winds in winter are similar to those in autumn. The columnar aerosol properties over East China were strongly influenced by the stationary regional meteorological conditions and the associated transport of anthropogenic aerosols from central China to the downwind regions. As a result, aerosols generated in coastal industrial regions worsened the air quality both local and in downwind regions. These aerosols were transported by the relatively

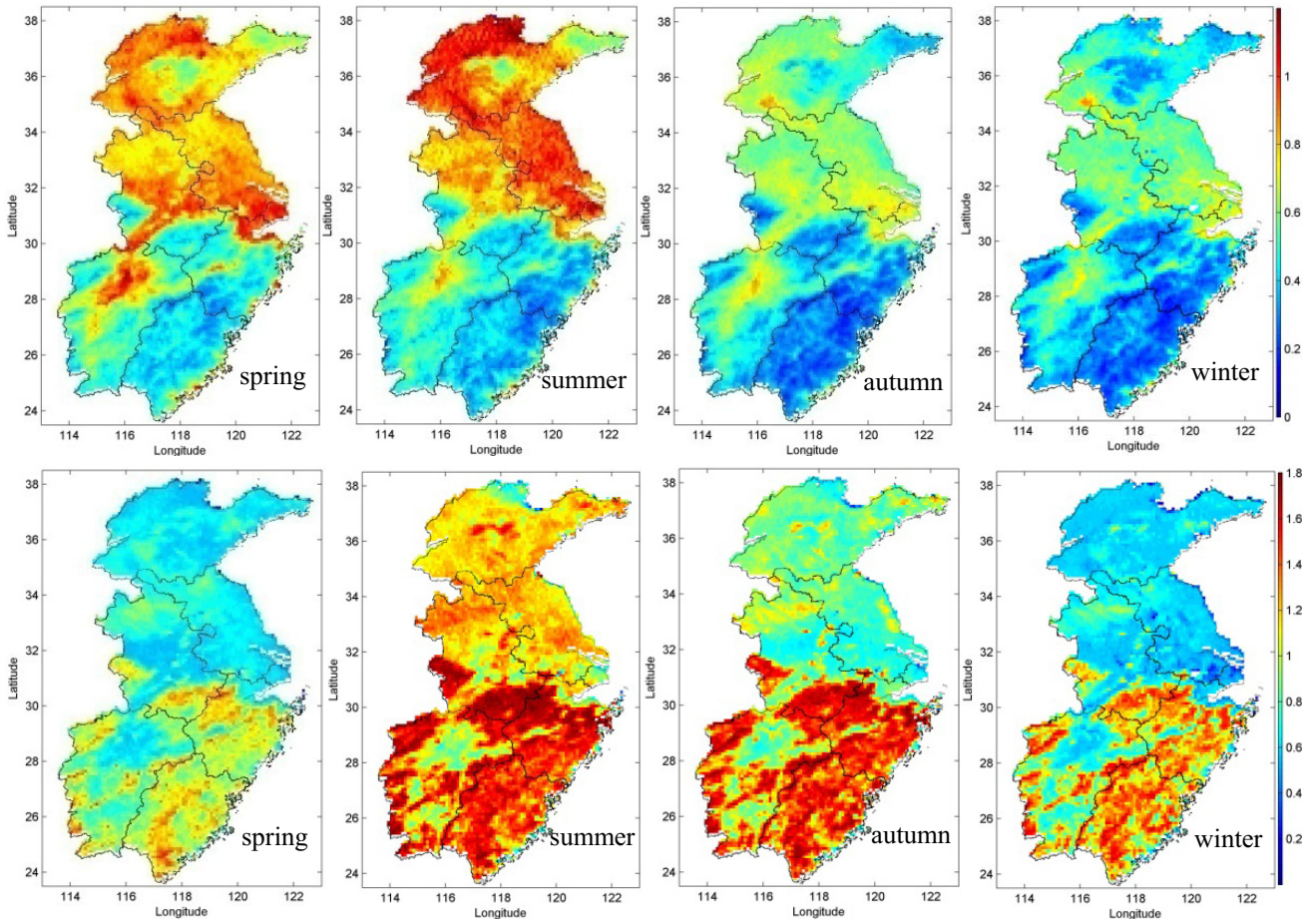

Fig. 5. The distribution of seasonal mean AOD (upper panel) and α (lower panel) over East China from the MODIS L2 product between 2000 and 2007.

low speed wind under stable atmospheric conditions, causing accumulations of aerosols. Formation of secondary fine particles through gas-to-particle conversion increased due to higher solar flux in summer. Lee *et al.* (2006) measured high AOD values over eastern China in summer due to burning. Although precipitation reduces aerosol loading, increased photo chemical reaction rate combined with anthropogenic emissions are also important source terms in summer.

Seasonally spatial distributions in MODIS derived AOD from 2000 to 2007 showed that the AOD maximum appeared in summer over the northern part of East China, which is quite different from the conclusion by Liu *et al.* (2003) who used the MODIS derived AOD from 2001 to 2002 and found the AOD maximum appeared in spring. According to Duan and Mao (2007), the dust days and area under its influence decreased gradually from 2000 to 2004. A time series of seasonally mean AOD over YRD from 2000 to 2007 can clearly validate the transformation of AOD maximum from spring to summer as shown in Fig. 6. The mean AODs in spring are significantly higher than that in summer from 2000 to 2002. The aerosol loadings in spring began to decrease and that in summer keep increasing or steady since 2003, which result in the seasonally mean AODs in spring are less than that in summer, especially for the year from 2003 to 2006. Therefore, it may be considered that the Asia dust weakened over the past, and possibly led to the AOD maximum shifting from spring to summer.

Aerosol Characteristics over Typical Regions in East China

Zone I, II and III with area of 100 × 100 km^2 in East China were selected according to aerosol source and local meteorological condition and were shown in Fig. 1. Zone I is more frequently influenced by Asian dust, Zone II is the typical urban/industrial region, and Zone III represents the natural background with dominant continental and marine aerosol. MODIS-derived AODs are averaged in each Zone and the meteorological data such temperature, RH, wind direction are obtained from the meteorological station located in the centre of each Zone. The meteorological data corresponding to the time when MODIS passed over are used to study the impact of meteorological factors to aerosol distribution and properties.

AOD at a particular location depends on a number of factors, including aerosol burden throughout the atmospheric column, aerosol size distributions, and its chemical composition (as it relates to the amount of water uptake and refractive index). Table 2 lists monthly and seasonal mean MODIS-derived AODs over each zone. The results clearly

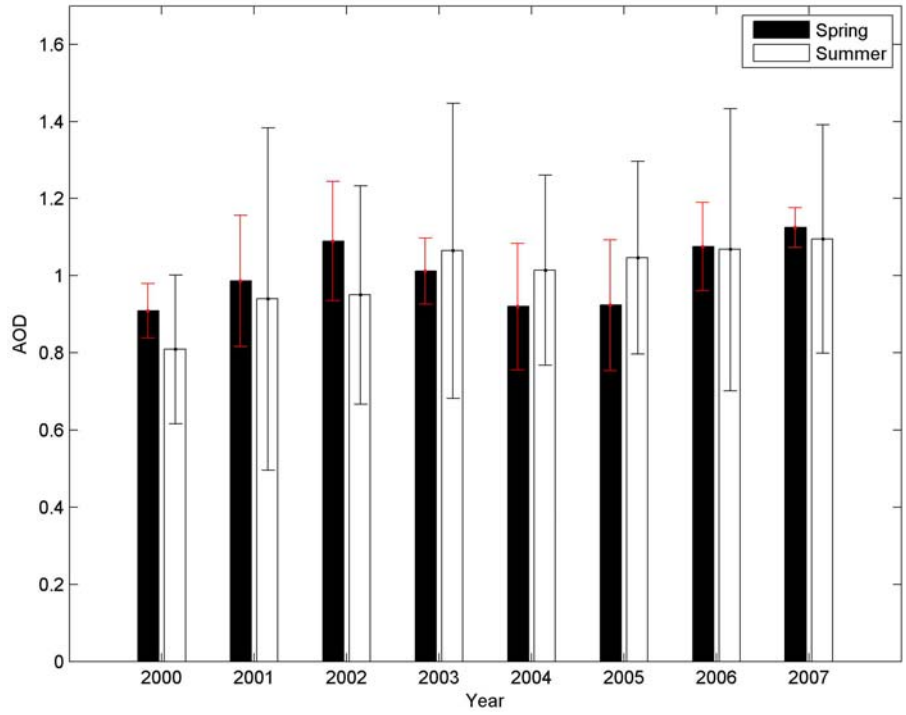

Fig. 6. The temporal variation of seasonally mean AOD over YRD from 2000 to 2007 for Spring and Summer, respectively. The errorbars respresent the standard deviations.

Table 2. The monthly and seasonal mean AOD and FMF in the three zones from the MODIS L2 product between 2000 and 2007. The numbers in the parentheses are the standard bias.

Region	I		II		III	
Month	AOD	FMF	AOD	FMF	AOD	FMF
Jan	0.47(0.26)	19.4(34.1)	0.62(0.23)	32.3(42.8)	0.32(0.19)	58.1(33.3)
Feb	0.60(0.39)	8.7(22.2)	0.73(0.31)	15.8(29.9)	0.36(0.19)	64.0(29.9)
Mar	0.83(0.49)	13.7(26.4)	0.90(0.39)	21.0(33.4)	0.48(0.29)	51.5(34.3)
Apr	1.05(0.58)	17.9(28.0)	1.03(0.37)	23.4(33.6)	0.51(0.28)	52.0(37.4)
May	1.12(0.68)	19.8(29.3)	1.08(0.44)	23.6(31.8)	0.44(0.22)	65.6(34.5)
Jun	1.37(0.65)	33.7(34.5)	1.28(0.48)	42.2(34.3)	0.47(0.32)	81.5(26.0)
Jul	1.26(0.96)	72.4(31.5)	0.98(0.54)	65.9(34.2)	0.35(0.23)	81.0(28.8)
Aug	0.87(0.69)	76.8(28.6)	0.77(0.53)	70.3(30.2)	0.40(0.25)	84.9(26.0)
Sep	0.77(0.65)	55.8(33.3)	0.72(0.39)	53.2(35.1)	0.35(0.23)	90.7(16.6)
Oct	0.71(0.56)	28.7(35.3)	0.70(0.34)	19.0(31.0)	0.34(0.22)	79.3(26.0)
Nov	0.51(0.32)	14.4(27.4)	0.67(0.28)	16.2(28.4)	0.30(0.24)	67.4(30.8)
Dec	0.42(0.25)	12.8(27.2)	0.61(0.25)	19.2(32.1)	0.25(0.21)	65.8(32.0)
Spring	1.01(0.61)	17.4(28.1)	1.01(0.41)	22.7(32.9)	0.48(0.27)	56.2(36.0)
Summer	1.17(0.81)	60.7(37.2)	0.99(0.56)	61.2(34.8)	0.39(0.26)	82.4(27.3)
Autumn	0.67(0.54)	33.3(36.5)	0.70(0.34)	28.6(35.5)	0.33(0.23)	79.1(26.8)
Winter	0.49(0.31)	13.5(28.4)	0.66(0.27)	21.5(35.1)	0.30(0.20)	62.8(31.9)

indicate that seasonal mean AOD is considerably higher during spring and summer than in winter, with minimum values in December for all zones. It is interesting to note that the standard bias of AOD in Spring and Summer are usually higher than that in winter, which indicate that more frequent variation of aerosol loading caused by Asian dust transportation in Spring and the wet removals in Summer. More detailed explanation about the variation of aerosol loading in different season can be found in section 3.4. Monthly mean AODs in zone I and II were usually larger than 0.5 with minimum values of 0.42 ± 0.25 and 0.61 ± 0.25, respectively. In zone I, AOD maximum of 1.37 ± 0.65 was found in June, and the FMFs range from 8.7 to 76.8 with maximum of 76.8 ± 28.6 in August. FMFs are lowest in February, when the coarse mode particles dominate in the atmosphere column. The enhanced turbidity in June was due to the formation of fine particles through gas-to-particle conversion process and the stronger turbulent that lifts

aerosol particles near the surface into atmosphere.

Based on the aircraft-based, ship-based and ground-based measurements during ACE-Asia, Buzorius *et al.* (2004) reported the secondary aerosol formation in Asian continental outflows. They found elevated concentrations of aerosol particles in the nucleation mode, with subsequent growth in the Aitken mode from ground-based aerosol size distribution measurements. From hygroscopicity measurements, they also concluded that newly formed aerosol particles mainly consisted of ammonium sulfate. Aircraft-based measurement data showed a layer of enlarged SO_2 concentration coinciding with an increased aerosol total number concentration. As additional circumstantial evidence, Yamaji *et al.* (2006) reported that the boundary layer O_3 concentrations in May and June were highest in the area stretching from East China to Japan. They also estimated that 30–60% of O_3 in May–June were produced by photo-chemical process through local anthropogenic emissions. Moreover, hygroscopic growth of fine hydrophilic aerosols due to the enhanced relative humidity in the lower troposphere may contribute to the peak AOD in June. Previous studies showed that the eastern Asian atmosphere has large amount of sulfate, carbon and ammonium aerosols. For example, Kim *et al.* (2006) showed that the hygroscopic growth of Asian aerosols was much higher than that in Europe and the eastern US. AOD in zone II experienced a decrease from 1.28 ± 0.48 in June to 0.77 ± 0.53 after heavy rain fall in August with the monthly mean precipitation of 87.5 mm (as shown in Fig. 7), due to the wet removal. FMFs increased to its maximum in the same period, indicating that the wet deposition by precipitation or wet removal is an important aerosol sink. On one hand, the wet deposition is more effective for removing large aerosol particles from the air than those particles in accumulation mode. On the other hand, the fine particles produced by active gas-to-particle conversion process in summer might contribute to increase FMFs.

In zone III, monthly mean AOD increased to its maximum in April and decreased to minimum in December. The seasonal mean AOD in this region reached maximum in spring, which was distinctly different from other regions. This seasonal variation of AOD may be a result of the dominant natural background in zone where aerosol regional transportation significantly influenced local aerosol seasonal cycle. It is interesting to note that the seasonal variation of AOD and FMF in zone III was not as large as that in the other regions, and usually larger FMF indicated that fine mode particles are dominant in the region.

The Impact of Meteorological Factors to Aerosol Distribution and Properties

The AOD-wind Dependence

Meteorological parameters such as temperature, RH and wind greatly influence aerosol particles in their formation, scattering, aging, transport and diffusion. Aerosol properties that can be modified by these processes include size distributions, refractive index and vertical distributions. Many early ground observations have demonstrated these effects (Shettle and Fenn, 1979; Horvath and Dellago, 1993).

Fig. 8 presents variations of AOD and α in the three zones according to wind direction and speed. It is clear that the impact of wind on aerosol loading in different zones is closely related to local and surrounding sources, as well as terrain. Higher AOD (> 1.6) and α (~1.4) can be associated with lower wind speed (< 4 m/s), which indicates that the local anthropogenic emissions are dominant in Zone I. The variation of AOD with wind in this zone is similar to that observation in urban region of Jordan (Hussein *et al.*, 2011). Strong southeasterly winds (~6 m/s) related to heavy aerosol loading (AOD > 1.2) due to numerous middle and small scale industries located in that area. Zone II located in YRD is characterized by urban/industrial regions with dense populations. Moderate wind regardless of wind direction

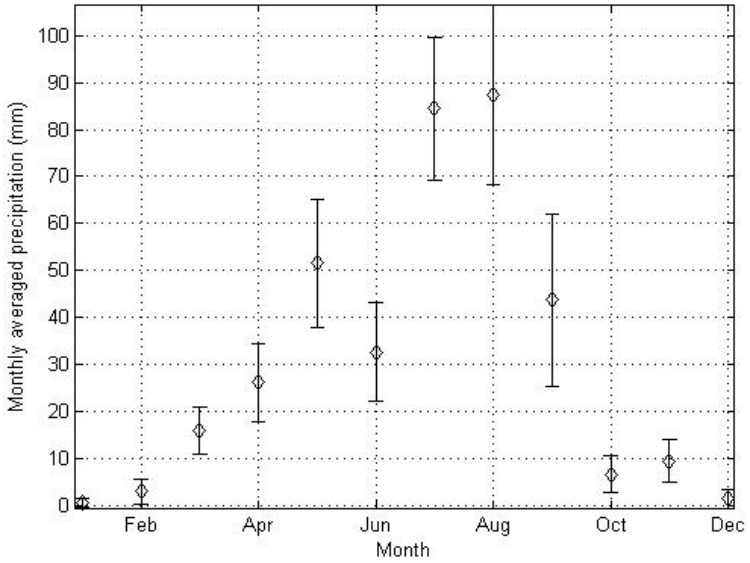

Fig. 7. The monthly averaged precipitation over zone II from 2000 to 2007. Rainfall within 24 hours prior to each valid observation as one sample, mean of the rainfall for all valid observations within each month for all years constitute the monthly averaged precipitation.

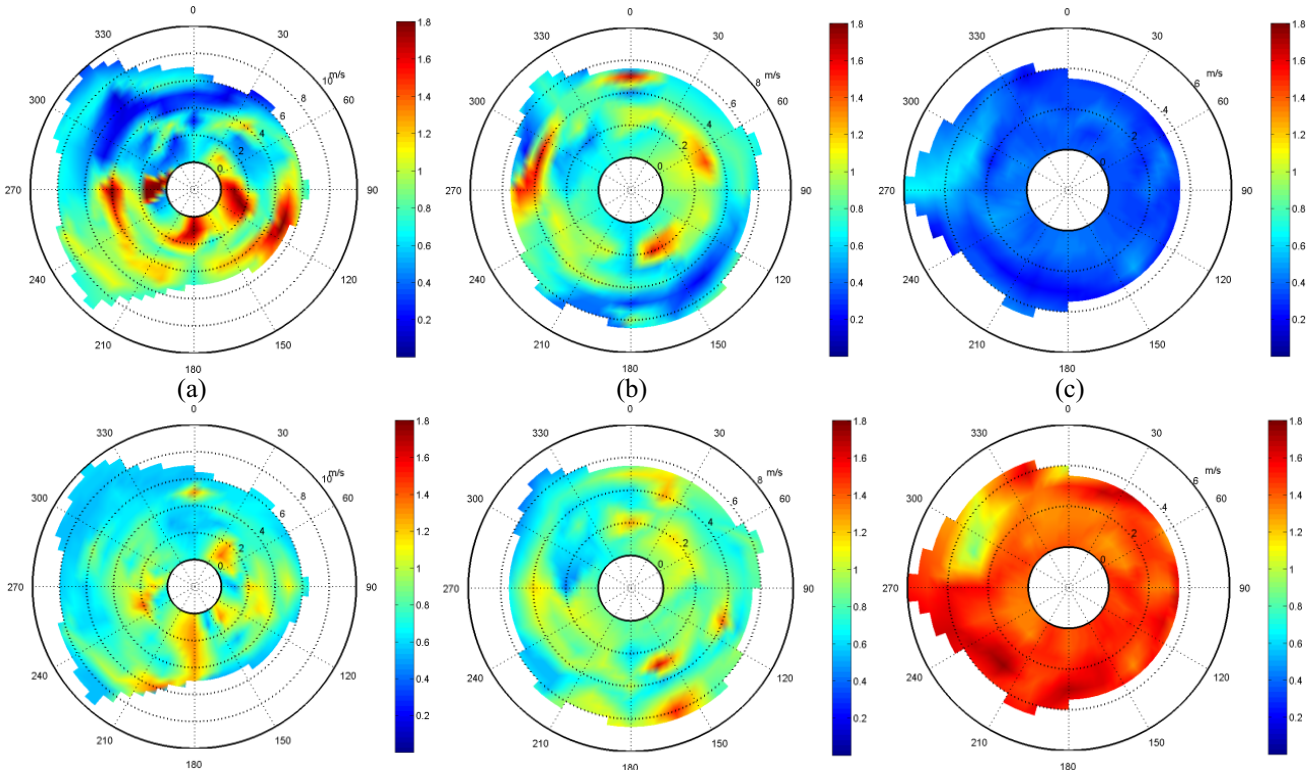

Fig. 8. The variation of AOD (up panel) and α (down panel) in zone (a)I, (b)II and (c)III according to the wind direction and wind speed.

brings abundant aerosol particles into this region. The easterlies brought fine urban/industrial aerosol from Shanghai downtown. Higher southeasterly wind (> 6 m/s) increased AOD up to 0.8, influenced by turbidity plumes from coastal cities in Zhejiang province. Regional aerosol transportation from Anhui province can significantly increase AOD in this zone when the westerly wind prevails.AOD in Zone III increased significantly up to 0.5 when the northwesterly wind speed reached between 3 and 6 m/s. The wind from other directions always brought aerosol particles characterized by AOD down to 0.3 or less and smaller size, which represent local aerosol characteristics. This result is similar to the observations by sun hazemeter in the Xishuangbanna station located in the tropical forests of Yunnan province in southwest China (Xin *et al.*, 2007). Colin *et al.* (2002) have suggested that the aerosol particle formation over forests is driven by biogenic gases and condensable organic vapors emitted by the vegetation. Therefore, it can be considered that this zone was usually influenced by the biogenic secondary organic aerosols formatted in continental luxuriant vegetation conditions through gas-to-particle conversion process.

The RH-aerosol Dependence

Fig. 9 shows the scattering plots between AOD and relative humidity (RH) in the three zones. In this figure, AOD increases with RH due to hygroscopic growth of fine hydrophilic aerosols. Studies have revealed that the influence of RH on physical and chemical properties of aerosols is complex. This is primarily due to the fact that increase in RH can enhance particle growth through condensation, coagulation and re-suspension. This leads to the increase in light scattering, either due to increase in particle sizes and/or increase in the particle number density. In this study, we adopted the Kasten-Hanel experiential formula to investigate the dependence of AOD on RH as follow,

$$\sigma = \sigma_0 (1 - RH)^{-\gamma} \quad (1)$$

where σ and σ_0 are the scattering coefficients corresponding to RH and dry condition, respectively. γ is the hygroscopic growth coefficient.

Regardless of the aerosol absorption and the discrepancy of aerosol hygroscopic growth in different height, Eq. (1) can be transformed as,

$$\tau = \tau_0 (1 - RH)^{-\gamma} \quad (2)$$

The dependence of AOD on RH in the three zones was fitted according to Eq. (2) and the fitted curves were plotted in Fig. 9. The hygroscopic growth coefficients γ are 1.3965, 0.615 and 0.3341; the slopes of fitted curves are 0.0234, 0.0135 and 0.0047; the correlation coefficients are 0.5495, 0.4401 and 0.3176 in zones (I–III) respectively. It is remarkable that the slope and γ in zone I are higher than those in the other zones, indicating more obvious hygroscopic growth and more sensitive aerosol properties on RH.

Plenty of urban/industrial aerosols are suspended over zones I and II. Urban/industrial aerosol model which represents strong pollution in urban areas includes insoluble,

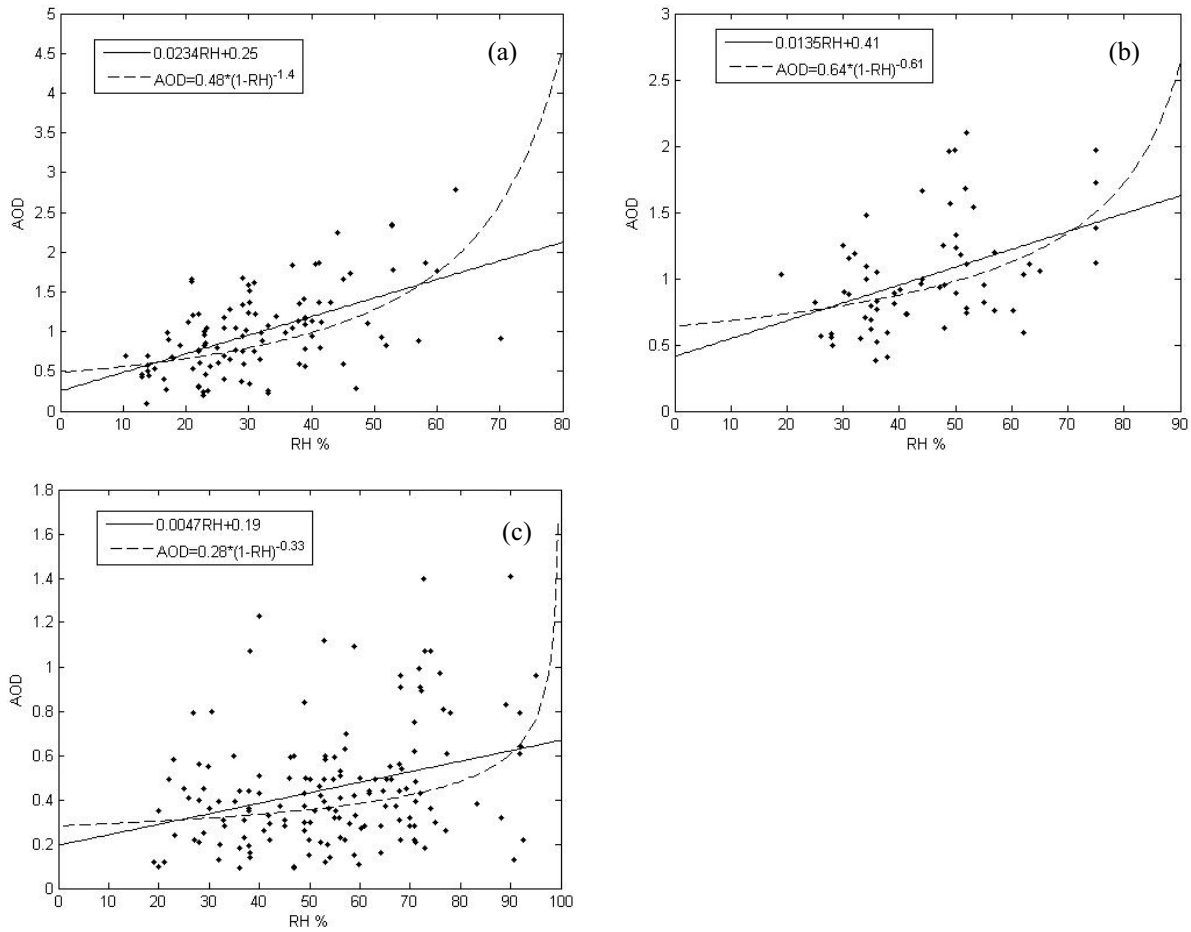

Fig. 9. The scattering dots between AOD and RH in spring over zone (a)I, (b)II and (c)III. The curve and line are the fitted results based on formula (2) and linearity respectively.

water soluble and soot aerosol species (Hess *et al.*, 1998). The insoluble aerosols are mostly soil particles with certain amount of organic material. The water soluble component that originated from gas to particle conversion contains various kinds of sulfate, nitrate, and other organics. In Table 3, the physical (mode radius and density) and optical (aerosol optical depth) properties of water soluble aerosol components for urban/industrial aerosol model as a function of relative humidity are given. The 550 nm AOD for urban/industrial aerosol model increases more than 3 folds when RH increases from 0% to 95%.

Table 3. Physical (Mode Radius, r_m, and Density, r, of Water Soluble Aerosol Component) and Optical (Aerosol Optical Depth (AOD) at 550 nm) Properties for Urban Aerosol Model (Hess *et al.*, 1998) as a Function of Relative Humidity (RH) varying from 0 to 95%.

RH %	r_m μm	ρ g/cm^3	τ (550 nm)
0	0.0212	1.80	0.362
50	0.0262	1.42	0.484
70	0.0285	1.33	0.560
80	0.0306	1.27	0.643
90	0.0348	1.18	0.849
95	0.0399	1.12	1.178

AOD-temperature Dependence

Correlation coefficient of AOD-T in the three zones was calculated according to different seasons. The result showed that the correlation coefficient of AOD-T for all samples in zone I is 0.3475, but it increases up to 0.5279 for winter, which is much higher than other zones.

Fig. 10 shows the variation of AOD with temperature confined by season and wind condition. The prevailing wind directions in different season determine the confine standard of wind condition and the limitation of wind speed is to ensure the simplification of aerosol source and type. '•' represents conditions where wind speed is less than 8 m/s and wind direction is between 60 and 90, where the correlation coefficient of AOD-T was 0.6663. 'o' represents conditions with wind speed of 4–5 m/s and wind direction between 190 and 220, where the correlation coefficient of AOD-T was 0.8913. '∆' represents conditions with wind speed of 1–3 m/s and wind direction between 190 and 240, where the correlation coefficient of AOD-T was 0.7875. '□' represents conditions where wind speed is less than 1 m/s and wind direction is between 190 and 300, where the correlation coefficient of AOD-T was 0.9236. '+' represents conditions where wind speed is less than 5 m/s and wind direction is between 200 and 290, where the correlation coefficient of AOD-T was 0.6941. '*' represents conditions

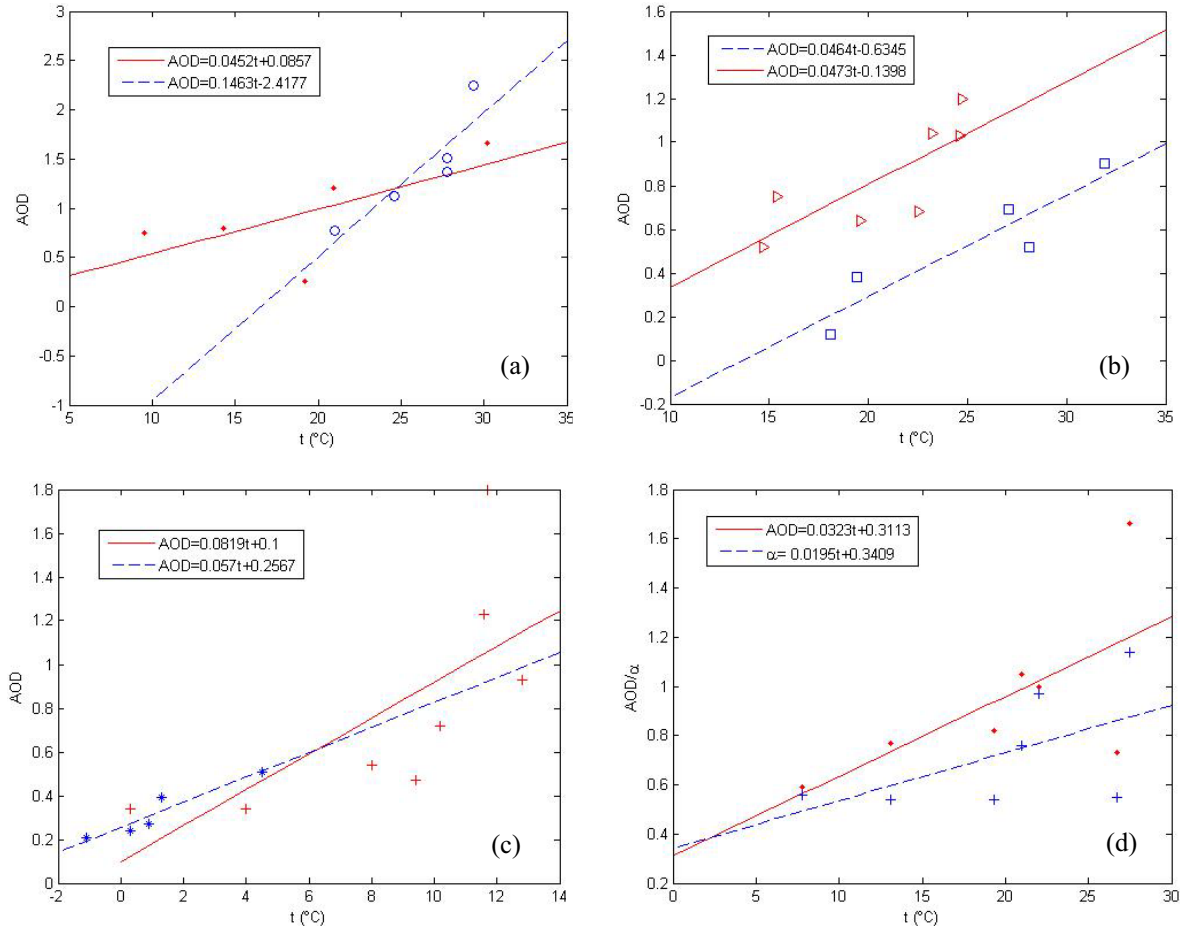

Fig. 10. The scattering dots between AOD and temperature in zone I for (a) spring, (b) autumn and (c) winter. (d) The scattering dots between AOD/α and temperature in zone II for spring. The curves are the fitted lines.

with wind speed of 1–5 m/s and wind direction between 300 and 360, where the correlation coefficient of AOD-T was 0.9473. In Fig. 10(d), '•'and '+' are the comparison of AOD and α versus temperature at wind speed less than 5 m/s and wind direction between 100 and 200, and the solid and dashed line are the fitted line for AOD and α, the correlation coefficient of AOD-T and α-T are 0.6514 and 0.5639, the slopes of fitted lines are 0.0323 and 0.01956, respectively. These comparisons indicate that AOD and α usually increase with the enhanced temperature, which is related to the atmospheric photochemical effect such as gas-particle conversion process. The increasing temperature accompanied by enhanced solar radiation is in favour of gas-particle conversion process and produces more fine mode particles. Furthermore, aerosols from different sources have different photochemical processes because of their different chemical components.

CONCLUSIONS

We present results of aerosol spatial distributions, seasonal and inter-annual variability, and the influence of meteorological conditions on aerosol physical properties derived from MODIS over East China from 2000 to 2007. High AOD are found in four regions in northwest plain including Shandong province, Huanghuai, Poyang Lake Plain and the Yangtze River Delta region (particularly the vicinity around the Yangtze River), with relative abundant coarse mode particles in the atmospheric column.

The dominant aerosols over the southern part of East China (excluding the Poyang Lake plain) are possibly continental and marine types. The dominant aerosols over the northern part of East China are possibly soil dust, biomass burning and urban/industrial pollutants. AODs show an increasing trend during the eight-year period, except for the years of 2004 and 2005 when the AOD over Shandong slightly decreased compared with that in 2003. The zone with AOD > 1.0 have been expanding during these years, especially after 2005. Of the high aerosol loading districts, the increase of annual mean AOD in YRD was fastest from 2000 to 2007, where large AOD extends more to the northward than southward. The peak AODs were mostly located in the big cities in northern parts of YRD from 2000 to 2007. Moreover, aerosol loading over the northern part increased more obviously than that over the southern part of East China. In spring, the AOD maxima appeared over Huaihe district and Poyang Lake plain. Maximum AOD in summer (up to 1.0) over YRD is caused by an increase of anthropogenic aerosols as well as a stagnant synoptic meteorological system dominant in Asian continent, causing

a build-up of pollutants in this region. Seasonal variations of derived MODIS AOD from 2000 to 2007 showed that the AOD maximum appeared in summer over YRD, which is quite different from a previous study by Liu *et al.* (2003). They found that the AOD maximum appeared in spring using the derived MODIS AOD from 2001 to 2002. The reason may be that Asian dust weakened, possibly leading to the maximum AOD shifting from spring to summer.

Three zones with area of 100 × 100 km^2 in East China were selected according to aerosol source and local meteorological condition. Monthly mean AODs in zone I and II were usually larger than 0.5. In these zones, AOD maximum was found in June and FMFs are lowest in February, when the coarse mode particles dominate in the atmosphere column. The enhanced turbidity in June was due to the formation of fine particles through gas-to-particle conversion process and the stronger turbulent that lifts aerosol particles near the surface into atmosphere. In zone III, monthly mean AOD increased to its maximum in April and decreased to minimum in December, which was distinctly different from other regions and may be a result of the dominant natural background in zone where aerosol regional transportation significantly influenced local aerosol seasonal cycle. Meteorological parameters such as temperature, RH and wind can greatly influence aerosol loadings, with different effects on different aerosol sources.

ACKNOWLEDGMENTS

The study is partially supported by the research grants from the National Natural Science Foundation of China (NSFC, Grant Numbers: 40705013, 40775002, 40975012 and 41175020), the National High Technology Research and Development Program of China (863 Major Project, No. 2011AA12A104), the Shanghai Science and Technology Committee Research Special Funds (Grant Number: 10JC1401600, 10231203803 and 10231203900) and the China Meteorological Bureau Public Welfare Special Funds (Grant Number: GYHY(QX)200706019 and GYHY201106023). The authors gratefully acknowledge the MODIS Science Data Support Team and the Earth Observing System Data Gateway for processing and distributing MODIS data used in this paper, respectively. We would like to thank the two anonymous reviewers, whose useful comments have improved the paper.

REFERENCES

Barnaba, F. and Gobbi, G.P. (2004). Aerosol Seasonal Variability over the Mediterranean Region and Relative Impact of Maritime, Continental and Saharan Dust Particles over the Basin from MODIS Data in the Year 2001. *Atmos. Chem. Phys.* 4: 2367–2391, doi: 10.5194/acp-4-2367-2004.

Bian, H., Tie, X.X., Cao, J.J., Ying, Z.M., Han, S.Q. and Xue, Y. (2011). Analysis of a Severe Dust Storm Event over China: Application of the WRF-Dust Model. *Aerosol Air Qual. Res.* 11: 419–428, doi: 10.4209/aaqr.2011.04.0053

Buzorius, G., McNaughton, C.S., Clarke, A.D., Covert, D.S., Blomquist, B., Nielsen, K., and Brechtel, F.J. (2004). Secondary Aerosol Formation in Continental Outflow Conditions during ACE-Asia. *J. Geophys. Res.* 109: D24203, doi: 10.1029/2004JD004749.

Charlson, R.J., Schwartz, S.E., Hales, J.M., Cess, R.D., Coakley, J.A., Hansen, J.E. and Hofmann, D.J. (1992). Climate Forcing by Anthropogenic Aerosols. *Science* 255: 423–430.

Che, H.Z., Yang, Z.F., Zhang, X.Y., Zhu, C.Z., Ma, Q.L., Zhou, H.G. and Wang, P. (2009). Study on the Aerosol Optical Properties and their Relationship with Aerosol Chemical Compositions over Three Regional Background Stations in China. *Atmos. Environ.* 43: 1093–1099, doi: 10.1016/j.atmosenv.2008.11.010

Chu, D.A., Kaufman, Y.J., Zibordi, G., Chern, J D., Mao, J., Li, C, and Holben, B.N. (2003). Global Monitoring of Air Pollution over Land from the Earth Observing System-Terra Moderate Resolution Imaging Spectroradiometer (MODIS). *J. Geophys. Res.* 108: 4661, doi: 10.1029/2002JD003179.

Chu, D.A., Remer, L.A., Kaufman, Y.J., Schmid, B., Redemann, J., Knobelspiesse, K., Chern, J.D., Livingston, J., Russell, P.B., Xiong, X. and Ridgway, W. (2005). Evaluation of Aerosol Properties over Ocean from Moderate Resolution Imaging Spectroradiometer (MODIS) during 10 ACE-Asia. *J. Geophys. Res.* 110: D07308, doi: 10.1029/2004JD005208.

Colin, D.O., Aalto, P., Hämeri, K., Kulmala, M. and Hoffmann, T. (2002). Atmospheric Particles from Organic Vapours. *Nature* 416: 497–498

Duan, J. and Mao, J.T. (2007). Study on the Distribution and Variation Trends of Atmospheric Aerosol Optical Depth over the Yangtze River Delta. *Acta Sci. Circumst.* 27: 537–543.

Dubovik, O., Holben, B.N., Eck, T.F., Smirnov, A., Kaufman, Y.J., King, M.D., Tanre, D. and Slutsker, I. (2002). Variability of Absorption and Optical Properties of Key Aerosol Types Observed in Worldwide Locations. *J. Atmos. Sci.* 59: 590–608.

Guo, J.P., Zhang, X.Y., Wu, Y.R., Zhaxi, Y.Z., Che, H.Z., La, B., Wang, W. and Li, X.W. (2011). Spatio-temporal Variation Trends of Satellite-based Aerosol Optical Depth in China during 1980-2008, *Atmos. Environ.* 45: 6802–6811, doi: 10.1016/j.atmosenv.2011.03.068

Hatakeyama, S., Hanaoka, S., Ikeda, K., Watanabe, I., Arakaki, T., Sadanaga, Y., Bandow, H., Kato, S., Kajii, Y., Sato, K., Shimizu, A. and Takami, A. (2011). Aerial Observation of Aerosols Transported from East Asia — Chemical Composition of Aerosols and Layered Structure of an Air Mass over the East China Sea. *Aerosol Air Qual. Res.* 11: 497–507, doi: 10.4209/aaqr.2011.06.0076.

Haywood, J.M. and Boucher, O. (2000). Estimates of the Direct and Indirect Radiative Forcing Due to Tropospheric Aerosol: A Review. *Rev. Geophys.* 38: 513–543.

He, Q.S., Li, C.C., Mao, J.T., Lau, A.K.H. and Li, P.R. (2006). A Study on the Aerosol Extinction-to-backscatter Ratio with Combination of Micro-pulse LIDAR and MODIS over Hong Kong. *Atmos. Chem. Phys.* 6: 3243–

3256, doi: 10.5194/acp-6-3243-2006.

He, Q.S., Li, C.C., Tang, X., Li, H.L., Geng, F.H. and Wu, Y.L. (2010). Validation of MODIS Derived Aerosol Optical Depth over the Yangtze River Delta in China. *Remote Sens. Environ.* 114: 1649–1661, doi: 10.1016/j.rse.2010.02.015.

Hess, M., Koepke, P. and Schult, I. (1998). Optical Properties of Aerosols and Clouds. The Software Package OPAC. *Bull. Am. Meteorol. Soc.* 79: 831–844.

Horvath, H. and Dellago, C. (1993). On the Accuracy of the Size Distribution Information Obtained from Light Extinction and Scattering Measurements: II. Case Studies. *J. Aerosol Sci.* 24: 143–154.

Huebert, B.J., Bates, T., Russell, P.B., Shi, G., Kim, Y.J., Kawamura, K., Carmichael, G. and Nakajima, T. (2003). An Overview of ACE-Asia. Strategies for Quantifying the Relationships 30 between Asian Aerosols and their Climatic Impacts. *J. Geophys. Res.* 108: 8633, doi: 10.1029/2003JD003550.

Hussein, T., Rasha, A., Tuukka, P., Heikki, J., Arafah, D., Kaarle, H. and Markku, K. (2011). Local Air Pollution versus Short–range Transported Dust Episodes: A Comparative Study for Submicron Particle Number Concentration. *Aerosol Air Qual. Res.* 11: 109–119, doi: 10.4209/aaqr.2010.08.0066

Hutchison, K.D., Smith, S. and Faruqui, S.J. (2005). Correlating MODIS Aerosol Optical Thickness Data with Ground-based $PM_{2.5}$ Observations across Texas for Use in a Real-time Air Quality Prediction System. *Atmos. Environ.* 39: 7190–7203.

IPCC (2001). Climate Change 2001: *The Scientific Basis, Contribution of Working Group I to the Third Assessment Report of the Inter governmental Panel on Climate Change,* Houghton, J.T., Ding, Y., Griggs, D.J., Noguer, M., Van der Linden, P.J., Dai, X., Maskell, K. and Johnson, C.A., (Eds.), Cambridge Univ. Press, New York, p. 349–416.

Kaufman, Y.J., Tanre, D.L., Remer, A., Vermote, E.F., Chu, A. and Holben, B.N. (1997). Operational Remote Sensing of Tropospheric Aerosol over Land from EOS Moderate Resolution Imaging Spectroradiometer. *J. Geophys. Res.* 102: 17051–17067.

Kaufman, Y.J., Tanre, D., Leon, J.F. and Pelon, J. (2003). Retrievals of Profiles of Fine and Coarse Aerosols Using Lidar and Radiometric Space Measurements. *IEEE Trans. Geosci. Remote Sens.* 41: 1743–1754.

Kim, J., Yoon, S.C., Jefferson, A. and Kim, S.W. (2006). Aerosol Hygroscopic Properties during Asian Dust, Pollution, and Biomass Burning Episodes at Gosan, Korea in April 2001. *Atmos. Environ.* 40: 1550–1560.

Kim, S.W., Yoon, S.C., Jefferson, A., Ogren, J.A., Dutton, E.G., Won, J.G., Ghim, Y.S., Lee, B.I. and Han, J.S. (2005). Aerosol Optical, Chemical and Physical Properties at Gosan, Korea during Asian Dust and Pollution Episodes in 2001. *Atmos. Environ.* 39: 9–50.

Kim, S.W., Yoon, S.C., Kim, J.Y. and Kim, S.Y. (2007). Seasonal and Monthly Variations of Columnar Aerosol Optical Properties over East Asia Determined from Multi-year MODIS, LIDAR, and AERONET Sun/Sky Radiometer Measurements. *Atmos. Environ.* 41: 1634–1651, doi: 10.1016/j.atmosenv.2006.10.044.

King, M.D., Kaufman, Y.J., Menzel, W.P. and Tanre, D. (1992). Remote Sensing of cloud. Aerosol. and Water Vapor Properties from the Moderate Resolution Imaging Spectrometer (MODIS). *IEEE Trans. Geosci. Remote Sens.* 30: 2–27.

Kleidman, R.G., O'Neill, N.T., Remer, L.A., Kaufman, Y.J., Eck, T.F., Tanré, D., Dubovik, O. and Holben, B.N. (2005). Comparison of Moderate Resolution Imaging Spectroradiometer (MODIS) and Aerosol Robotic Network (AERONET) Remote-sensing retrievals of Aerosol Fine Mode Fraction over Ocean. *J. Geophys. Res.* 110: D22205, doi: 10.1029/2005JD005760.

Lee, K.H., Kim, Y.J. and Han, J.S. (2006). Characteristics of Aerosol Observed during Two Severe Haze Events over Korea in June and October 2004. *Atmos. Environ.* 40: 5146–5155.

Levine, J.S., Cofer, W.R., Cahoon, D.R. and Winstead, E.L. (1995). Biomass Burning: A Driver for Global Change. *Environ. Sci. Technol.* 29: 120–125.

Levy, R.C., Remer, L.A., Tanre, D., Kaufman, Y.J., Ichoku, C., Holben, B.N., Livingston, J.M., Russell, P.B. and Maring, H. (2003). Evaluation of the Moderate-Resolution Imaging Spectroradiometer (MODIS) Retrievals of Dust Aerosol over the Ocean during PRIDE. *J. Geophys. Res.* 108: 8594, doi: 10.1029/2002JD002460.

Levy, R.C., Remer, L.A., Mattoo, S., Vermote, E.F. and Kaufman, Y.J. (2007). Second-generation Operational Algorithm: Retrieval of Aerosol Properties over Land from Inversion of Moderate Resolution Imaging Spectroradiometer Spectral Reflectance. *J. Geophys. Res.* 112: D13211, doi: 10.1029/2006JD007811.

Li, H.Y., Han, Z.W., Cheng, T.T., Du, H.H., Kong, L.D., Chen, J.M., Zhang, R.J. and Wang, W.J. (2010). Agricultural Fire Impacts on the Air Quality of Shanghai during Summer Harvesttime. *Aerosol Air Qual. Res.* 10: 95–101, doi: 10.4209/aaqr.2009.08.0049

Li, Z. (2004). Aerosol and Climate: A Perspective from East Asia, In *Observation, Theory and Modelling of the Atmospheric Variability*, Hackensack, N.J. (Ed.), World Sci, p. 501–525.

Liu, G.Q., Li, C.C., Zhu, A.H. and Mao, J.T. (2003). Optical Depth Research of Atmospheric Aerosol in the Yangtze River Delta Region. *Shanghai Environ. Sci.* appl. 58–63.

Luo, Y.F., Lu, D.R., Zhou, X.J., Li, W.L. and He, Q. (2001). Characteristics of the Spatial Distribution and Yearly Variation of Aerosol Optical Depth over China in Last 30 years. *J. Geophys. Res.* 106: 14501–14513.

Menon, S., Hansen, J.E., Nazarenko, L. and Luo, Y.F. (2002). Climate Effects of Black Carbon Aerosols in China and India. *Science* 297: 2249–2252.

Nakajima, T., Sekiguchi, M., Takemura, T., Uno, I., Higurashi, A., Kim, D., Sohn, B.J., Oh, S.N., Nakajima, T.Y., Ohta, S., Okada, I. and Takamura, T. (2003). Significance of Direct and Indirect Radiative Forcings of Aerosols in the East China Sea Region. *J. Geophys. Res.* 108: 8658, doi: 10.1029/2002JD003261.

Pan, L., Che, H.Z., Geng, F.H., Xia, X.G., Wang, Y.Q., Zhu, C.Z., Chen, M., Gao, W. and Guo, J.P. (2010). Aerosol Optical Properties Based on Ground Measurements over the Chinese Yangtze Delta Region. *Atmos. Environ.* 44: 2587–2596, doi: 10.1016/j.atmosenv.2010.04.013.

Pilinis, C., Pandis, S.N. and Seinfeld, J.H. (1995). Sensitivity of Direct Climate Forcing by Atmospheric Aerosols to Aerosol Size and Composition. *J. Geophys. Res.* 100: 18739–18754.

Qian, Y. and Giorgi, F. (2000). Regional Climatic Effects of Anthropogenic Aerosols? The Case of Southwestern China. *Geophys. Res. Lett.* 27: 3521–3524.

Ramachandran, S. (2007). Aerosol Optical Depth and Fine Mode Fraction Variations Deduced from Moderate Resolution Imaging Spectroradiometer (MODIS) over Four Urban Areas in India. *J. Geophys. Res.* 112. D16207, doi: 10.1029/2007JD008500.

Remer, L.A. and Kaufman, Y.J. (1998). Dynamic Aerosol Model: Urban/Industrial Aerosol. *J. Geophys. Res.* 103: 13859–13871.

Remer, L.A., Kaufman,Y.J., Tanre, D., Mattoo, S. Chu, D.A. Martins, J.V., Li, R., Ichoku, C., Levy, R.C. and Kleidman, R.G. (2005). The MODIS Aerosol Algorithm, Products and Validation. *J. Atmos. Sci.* 62: 947–973.

Shettle, E.P. and Fenn, R.W. (1979). *Models for the Aerosols of the Lower Atmosphere and the Effects of Humidity Variations on their Optical Properties*, AFGL-TR-79-0214, Air Force Geophys. Lab., Hanscom AirForce Base, Mass, p. 94.

Stone, E.A., Yoon, S.C. and Schauer, J.J. (2011). Chemical Characterization of Fine and Coarse Particles in Gosan, Korea during Springtime Dust Events. *Aerosol Air Qual. Res.* 11: 31–43, doi: 10.4209/aaqr.2010.08.0069

Tang, J., Xue, Y., Yu, T. and Guan, Y. (2005). Aerosol Optical Thickness Determination by Exploiting the Synergy of TERRA and AQUA MODIS. *Remote Sens. Environ.* 94: 327–334.

Xia, X.A., Chen, H.B., Wang, P.C., Zhang, W.X., Goloub, P., Chatenet, B., Eck, T.F. and Holben B.N. (2006). Variation of Column-integrated Aerosol Properties in a Chinese Urban Region. *J. Geophys. Res.* 111: D05204, doi: 10.1029/2005JD006203.

Xiao, Z.M., Zhang, Y.F, Hong, S.M., Bi, X.H., Jiao, L., Feng, Y.C. and Wang, Y.Q. (2011). Estimation of the Main Factors Influencing Haze, Based on a Long-term Monitoring Campaign in Hangzhou, China. *Aerosol Air Qual. Res.* 11: 873–882, doi: 10.4209/aaqr.2011.04.0052.

Xin, J.Y., Wang, Y.S., Li, Z.Q., Wang, P.C., Hao, W.M., Nordgren, B.L., Wang, S.G., Liu, G.R., Wang, L.L., Wen, T.X., Sun, Y. and Hu, B. (2005). Aerosol Optical Depth (AOD) and Angstrom Exponent of Aerosols Observed by the Chinese Sun Hazemeter Network from August 2004 to September 2005, *J. Geophys. Res.* 112: D05203, doi: 10.1029/2006JD007075.

Xu, J., Bergin, M.H., Yu, X., Liu, G., Zhao, J., Carrico, C.M. and Baumann, K. (2002). Measurement of Aerosol Chemical, Physical and Radiative Properties in the Yangtze Delta Region of China. *Atmos. Environ.* 36: 161–173.

Xu, Q. (2001). Abrupt Change of the Midsummer Climate in Central East China by the Influence of Atmospheric Pollution. *Atmos. Environ.* 35: 5029–5040.

Yamaji, K., Ohara, T., Uno, I., Tanimoto, H., Kurokawa, J., and Akimoto, H. (2006). Analysis of the Seasonal Variation of Ozone in the Boundary Layer in East Asia Using the Community Multi-scale Air Quality Model: What Controls Surface Ozone Levels over Japan? *Atmos. Environ.* 40: 1856–1868.

Yuan, S.Q. and Qian, H.S. (2003). Relations of Energy Consumption to Climate in China: A Statistical Analysis. *Meteorol. Sci. Technol.* 31: 29–32

Zhang, J.H., Si, S.J., Mao, J.T. and Wang, M.H. (2003). Remote Sensing Optical Depth over China with GMS-5 Satellite. *Chinese J. Atmos. Sci.* 27: 23–35.

Zhang, J.Y., Li, Y., Cai, X.N., Zou, X.K. and Qiao, L. (2010). Characteristics of Sand and Dust Weather in China and Cause Analysis in the Spring of 2006. *Meteorol. Mon.* 36: 59–65.

Received for review, November 4, 2011
Accepted, February 22, 2012